

We are IntechOpen, the world's leading publisher of Open Access books Built by scientists, for scientists

6,900

Open access books available

186,000

International authors and editors

200M

Downloads

Our authors are among the

154

Countries delivered to

TOP 1%

most cited scientists

12.2%

Contributors from top 500 universities



WEB OF SCIENCE™

Selection of our books indexed in the Book Citation Index
in Web of Science™ Core Collection (BKCI)

Interested in publishing with us?
Contact book.department@intechopen.com

Numbers displayed above are based on latest data collected.
For more information visit www.intechopen.com



Selection of Optimal Processing Condition during Removal of Methylene Blue Dye Using Treated Betel Nut Fibre Implementing Desirability Based RSM Approach

Amit Kumar Dey and Abhijit Dey

Abstract

Adsorption of Methylene Blue onto chemically (Na_2CO_3) treated ripe betel nut fibre (TRBNF) was studied using batch adsorption process for different concentrations of dye solutions (50, 100, 150 and 200 mg/L). Experiments were carried out as a function of contact time, initial solution pH (3 to 11), adsorbent dose (10 gm/L – 18 gm/L) and temperature (293, 303 and 313 K). The adsorption was favoured at neutral pH and lower temperatures. Adsorption data were well described by the Langmuir isotherm and subsequently optimised using a second-order regression model by implementing face-centred CCD of Response Surface Methodology (RSM). The adsorption process followed the pseudo-second-order kinetic model. The maximum sorption capacity (q_{max}) was found to be 31.25 mg/g. Thermodynamic parameters suggest that the adsorption is a typical physical process, spontaneous, enthalpy driven and exothermic in nature. The maximum adsorption occurred at pH 7.0. The effect of adsorption was studied and optimum adsorption was obtained at a TRBNF dose of 15 gm/L.

Keywords: Adsorption, Methylene Blue, betel nut fibre, RSM, Desirability

1. Introduction

Colour plays a significant importance in the human world as everybody likes colourful clothes, our food, medicine etc. is also having various colours. It is quite obvious that many researchers have carried out various studies on colour and its production. In this present situation, about ten thousand or more dyes are available commercially and the annual production of dye is about seven lakh tons [1]. There are numerous structural varieties available for dye like azo dye, acidic dye, basic dye, disperse, anthraquinone based and metal complex dyes. Dyes are mainly used in textile industries. A large portion of synthetic dyes do not bind during the process of colouration and it is then discharged to the waste streams [2]. The amount of dye that is discharged into the environment during the colouration process is about 10–15%. Those dyes discharge into waste streams are highly coloured and those are not pleasing aesthetically. Thus the textile industries cause the discharge

of a large number of dyes and other additives into the environment, produced during the dyeing process [3]. The conventional water treatment process is not found to be effective in the case of removal of these dyes. Due to their high solubility in water, dyes are easily transported through a sewer and it finally reaches the natural water bodies. Carcinogenic and products having high toxicity are produced by the degradation of these dyes [4]. These dyes may cause hazardous effects to living organism too. Special concern should be there to prevent the contamination caused by these dyes and to do this the quantity estimate of dyes discharged into natural bodies should be done properly. It is well known that the use of activated carbon for the treatment of wastewater (removal of dyes from wastewater) is a very well established technique, but due to the high cost involved in the process, researchers are constantly working on finding other low-cost bio-sorbents which are effective in the removal of dyes from wastewater [5–7]. In this work, we have attempted to use an agricultural product, chemically treated Ripe Betel Nut fibre (TRBNF) for the removal of a textile dye namely Methylene Blue (MB) from an aqueous solution. Azo dyes form covalent bonds with the fibres they colour, e.g. cotton, rayon, wool silk and nylon. Methylene Blue is a commercial cationic dye with chemical formula $C_{16}H_{18}ClN_3S$ and Molar weight = $319.9 \text{ g}\cdot\text{mol}^{-1}$. The functional groups present in the dye molecule react with the -OH, -SH and -NH₂ groups present in the fibre rich in cellulosic materials. Azo dyes are mostly preferred in the textile industries due to their fastness of the substrate. Understanding the process of kinetic and mass transfer is very essential for the design of an adsorption treatment system [8–14]. Several techniques and methodologies have been incorporated in order to removal of dyes. Eventually along with the experimental analysis, researchers were focused to identify the approximate solution of these problems using different mathematical modeling along with several multi criteria decision making approaches. Several studies have also been reported to the implementation of Response surface Methodology for improving the dye removal process by adjusting the process variables [15–17]. RSM is employed to remove ethylene blue dye using cheap adsorbent. The regression analysis has been used for the removal of colour of aqueous dye solution by using a novel adsorbent [18–23].

The approach of RSM can better predicts the impact of process variables on performance characteristics as well as it can be considered as a better option for optimization [24]. The CCD of RSM have been implemented for the design of experiments. In this study experimentation have been made to remove the methylene blue dye using treated betel nut fibre. Optimum adsorption capacities have been identified using the second order quadratic model of face centered RSM approach. The influence of each process variables and their percentage contribution on the developed quadratic model is explored with the help of ANOVA.

2. Materials and methods

It is known that components high in cellulose and hemicellulose composition are good in removing azo dyes from an aqueous solution (**Figure 1**). The composition of Ripe Betel Nut fibre consists of Cellulose (52.09%), Hemi-cellulose (12.04%), Lignin (22.34%), Fat and ash (5.94%) and Water-soluble matter (1.5%). Sun-dried ripe betel nut fibre was collected from the market and cut into sizes of 1 mm size and washed with distilled water and dried at 60°C thus raw betel nut fibre was obtained. The sample was then treated with 0.01 M Na₂CO₃ at room temperature for 4 hours, then distilled washed to remove excess chemicals in fibres and pH was reduced to 7, then dried for 4 hours at 100°C in a hot air oven and was kept in a container. Thus we get the treated ripe betel nut fibre (TRBNF). An azo dye Methylene

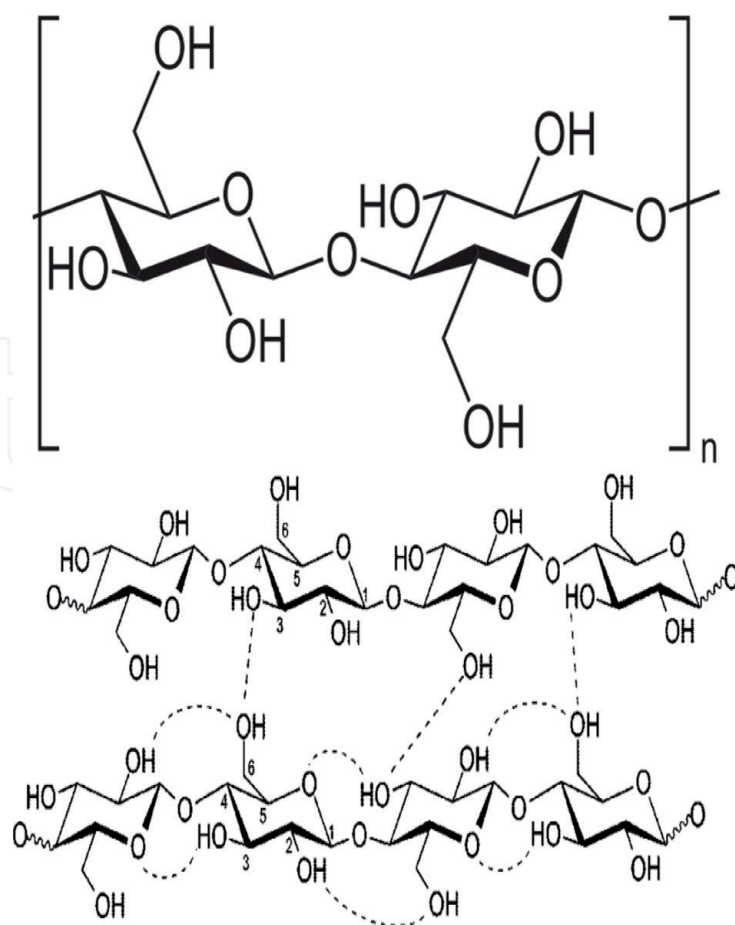


Figure 1.
(a) Cellulose structure; (b) Hydrogen bond structure of cellulose.

Blue, having a strong, though apparently non covalent, affinity to cellulose fibres, having molecular formula $C_{16}H_{18}ClN_3S$ was chosen as adsorbate. All the chemicals used were obtained from Himedia. A stock solution (1000 mg/L; pH 7) of dye was prepared using doubly distilled water.

3. Experiments and equilibrium studies

Batch adsorption studies were carried out and at first, the effect of pH variation on the removal of MB by TRBNF was studied and found that the maximum adsorption occurred at pH 7.0. From the stock solution of 1000 mg/L, different combinations of dye solutions were prepared for solutions of different initial concentrations viz. 50, 100, 150 and 200 mg/L at pH 7.0. Initial TRBNF dose was taken as 10 g/L and the same rate of the dose was mixed with each of the prepared solutions, agitated mechanically with the help of a rotary shaker at 303 K at 150 rpm until the equilibrium was reached. For time $t = 0$ minutes, 5 minutes, 10 minutes and so on, until equilibrium, the dye concentrations were measured by UV/VIS spectroscopy. The data were used to calculate the amount of dye adsorbed, q (mg/g). Effect of TRBNF dose was studied upon the absorption of MB dye by varying TRBNF dose at 10, 15 and 20 g/L. Experiments were carried out at different pH values ranging from 3 to 11. A fixed amount of TRBNF (1 gm) was added to the 100 ml of 50 mg/L of MB solution at different pH values (3–11) and agitated for 3 hours at 303 K to assess the influence of initial pH on MB concentration, by taking and measuring the samples after every five minutes of agitation. Experiments were also carried out to check for adsorption of MB by the container walls in the absence of betel nut fibre.

It was found that there was no degradation or adsorption of MB by container walls. Variation of temperature effect was evaluated for 293, 303 and 313 K. Experiments were carried out in duplicate and mean values were taken. The amount of dye adsorbed per unit adsorbent (mg dye per gm adsorbent) was calculated according to a mass balance on the dye concentration using the Eq. (1):

$$q_{\max} = \frac{(c_i - c_f)}{m} V \quad (1)$$

Where,

Q_{\max} = Maximum adsorption capacity (mg/g).

C_i = Initial concentration of dye in solution (mg/L).

C_f = Final concentration of dye in solution (mg/L).

V = Volume of solution (L).

m = adsorbent weight (g).

4. Adsorption studies by employing response surface methodology

Experiments were carried out batch-wise to obtain the maximum adsorption capacity (Q_{\max}) as a function of pH, Temperature (K), TRBNF dose (g/L) and rotational speed (RPM). Keeping the other process parameters as constant, the value of Q_{\max} was obtained once at a time by altering any one of the process parameters. Similarly, by using a combination of 30 different sets of a process parameter, the value of Q_{\max} was obtained 30 times and the values were utilized to obtain the most desirable condition, using response surface methodology. Response surface methodology (RSM) is used for the modelling and optimization of response characteristics with quantitative independent variables.

A regression model is also known as a polynomial quadratic model of order two as shown in Eq. (2) shows the system quality characteristic. The software 'Design Expert 11.0' gives an approximation of the regression model coefficient [22–26].

$$Y = C_0 + \sum_{i=1}^n C_i X_i + \sum_{i=1}^n d_i X_i^2 \pm \varepsilon \quad (2)$$

Face centered central composite second order design (CCD) technique was mainly used for the design experiment of the present study. The "face-centred CCD" possesses 30 combinations of 4 different process variables with 3 level of each [22–24]. **Tables 1** and **2** delineated the layout of process variables and the combination of 30 experimental runs obtained by RSM CCD experimental design approach.

The model fit summery demonstrated that the developed regression model is fit significantly for Q_{\max} on the selected experimental domain. The statistical analysis for the generated model has been demonstrated by the ANOVA analysis (**Table 3**). The model significance has been confined by the model F value. The probability of higher F value will be confirmed by value of model term less than 0.05 or in other words 95% confidence interval. It proves that the particular model terms are statistically significant for the developed model [20]. When the value of multiple coefficients of regression R_2 becomes unity, the response models fit better with actual data. The deviation becomes very less between the actual values and predicted values. The actual and predicted plots for Q_{\max} have been delineated in **Figure 2** demonstrating the degree of proximity of the model terms. The errors are normally

Parameters	Labels	Levels		
		-1	0	+1
Temperature, ($^{\circ}$ k)	A	293	303	313
TRBNF dose, (g/l)	B	10	14	18
pH.	C	3	7	11
Rotational speed, (RPM)	D	100	150	200

Table 1.
Operating variables and their levels.

Exp. no.	Factor1 A: pH	Factor 2 B: Temp	Factor 3 C: Jute Dose	Factor 4 D: RPM	Response Q_{\max} (mg/g)
1	3	313	10	200	10.21
2	3	293	10	100	11.42
3	11	293	18	200	15.67
4	3	313	10	100	5.19
5	11	313	18	100	10.43
6	3	313	18	200	12.69
7	3	293	10	200	11.76
8	11	293	10	200	11.28
9	7	303	14	150	28.91
10	11	313	10	200	11.19
11	11	313	10	100	11.01
12	7	303	14	150	28.78
13	7	303	14	150	29.56
14	3	293	18	100	12.64
15	3	293	18	200	16.34
16	11	313	18	200	13.41
17	11	293	10	100	11.29
18	11	293	18	100	13.38
19	3	313	18	100	11.31
20	7	303	14	150	29.59
21	7	303	14	150	29.19
22	7	303	14	150	29.49
23	7	303	14	100	27.48
24	3	303	14	150	24.91
25	7	303	10	150	27.21
26	7	293	14	150	32.11
27	7	313	14	150	30.38
28	7	303	14	200	28.19
29	7	303	18	150	31.56
30	11	303	14	150	27.87

Table 2.
Experimental results obtained with the setting of processing variables.

Source	Sum of Squares	df	Mean Square	F-value	p-value	
Model	20334.01	14	1452.43	21.85	< 0.0001	Significant
A-Temperature	341.82	1	341.82	5.14	0.0385	
B-TRBNF dose	472.47	1	472.47	7.11	0.0176	
C-pH	80.69	1	80.69	1.21	0.2879	
D-Rotational speed	261.14	1	261.14	3.93	0.0661	
AB	6.33	1	6.33	0.0952	0.7620	
AC	77.70	1	77.70	1.17	0.2967	
AD	20.21	1	20.21	0.3040	0.5895	
BC	84.36	1	84.36	1.27	0.2776	
BD	0.9702	1	0.9702	0.0146	0.9054	
CD	59.68	1	59.68	0.8978	0.3584	
A ²	168.79	1	168.79	2.54	0.1319	
B ²	434.59	1	434.59	6.54	0.0219	
C ²	1079.96	1	1079.96	16.25	0.0011	
D ²	658.42	1	658.42	9.91	0.0066	
Residual	997.02	15	66.47			
Lack of Fit	994.19	10	99.42	175.51	< 0.0001	Significant
Pure Error	2.83	5	0.5665			
Cor Total	21331.03	29				

Table 3.
The ANOVA results for Q_{max} .

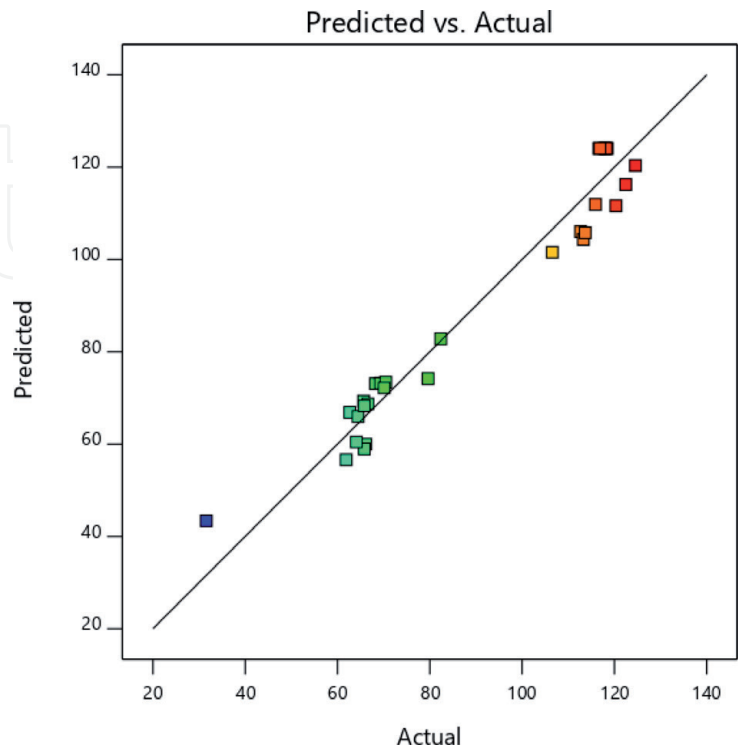


Figure 2.
Predicted vs. actual plot for Q_{max} .

distributed as a maximum of the values are close to a straight line. The standard normal distributions of the experimental data are obtained in the residual plots which validate the mathematical models [17, 19, 22]. The typical residual plots of the wear rates of composites are represented in **Figure 3**. The normal distribution of the data points in all the typical residual plots; normal probability plot (**Figure 3(a)**), Residual vs. run (**Figure 3(d)**); distribution of the predicted vs. Residual data points (**Figure 3(b)**); and the deficit vs. Run (**Figure 3(c)**) suggested that the residual and the predicted model for all the responses of the composites are observed to be distributed normally. The residuals are observed to be distributed near to the straight line revealing the normal distributions of the random errors. There were no unpredictable patterns observed on the residual plots as most of the run residues lie in between the range. The AP value was found to be 3. The comparison to the mean predicted error with the predicted value span at the design space can be represented by AP values arresting the adequate model discrimination [18, 26–30]. A larger values of AP (14.003) and coefficient of determination ($R_2 = 0.953$) have been predicted by the model for Q_{max} . Consequently, the insignificant lack of fit obtained for the developed model presumed that the generated model was best suited for selected operational domain for Q_{max} . It is possible to eliminate the insignificant model terms from the developed quadratic model and only the significant model terms would have been consider for the response surface for Q_{max} . A significant lack of fit was obtained due to retention of the insignificant model term in the developed model for Q_{max} (Eq. (3)). The developed surface model can be used to navigate

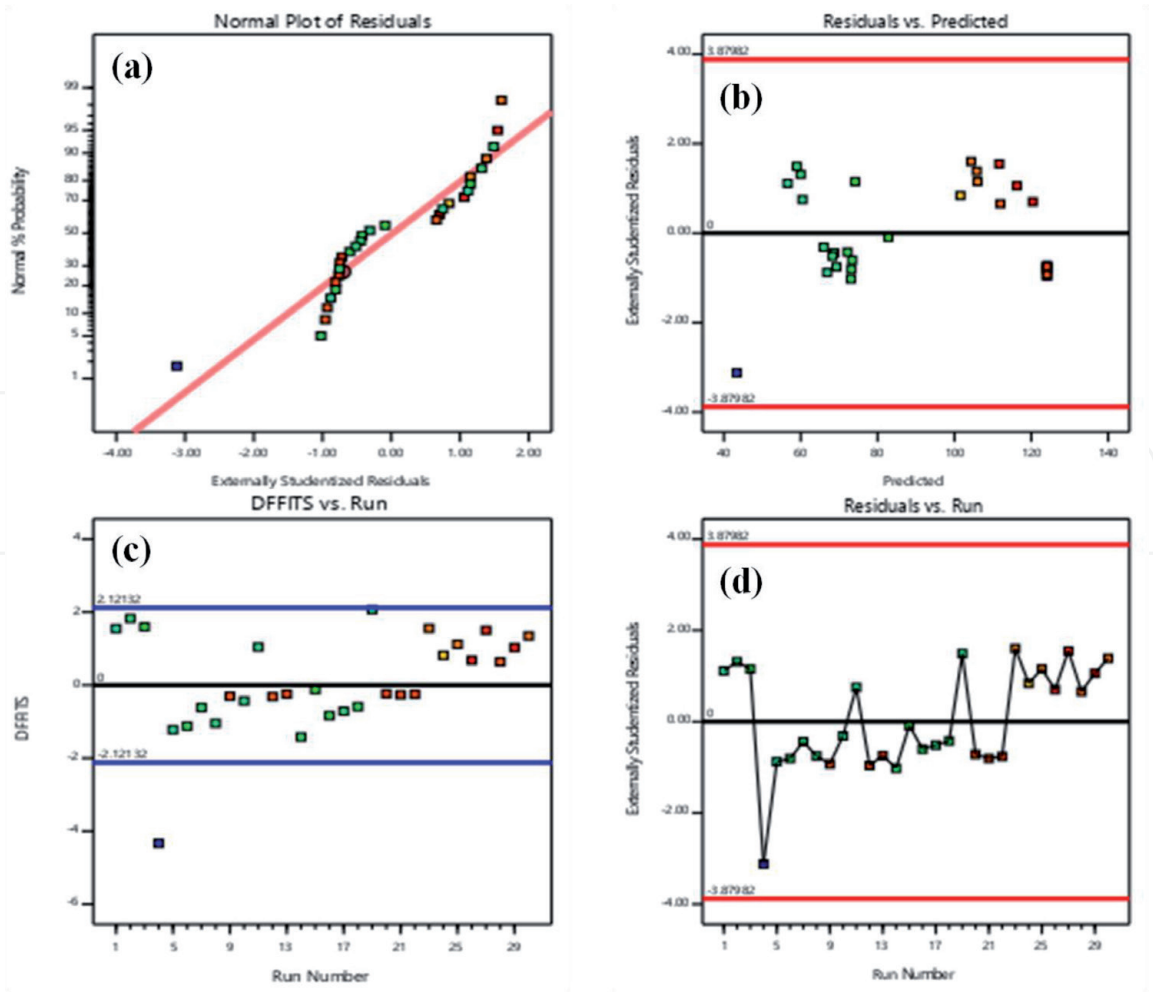


Figure 3. Model summary statistics for Q_{max} (a) Normal plots of Residuals; (b) Residuals Vs. Predicted; (c) Dffits Vs. Run; and (d) Residual Vs. Run.

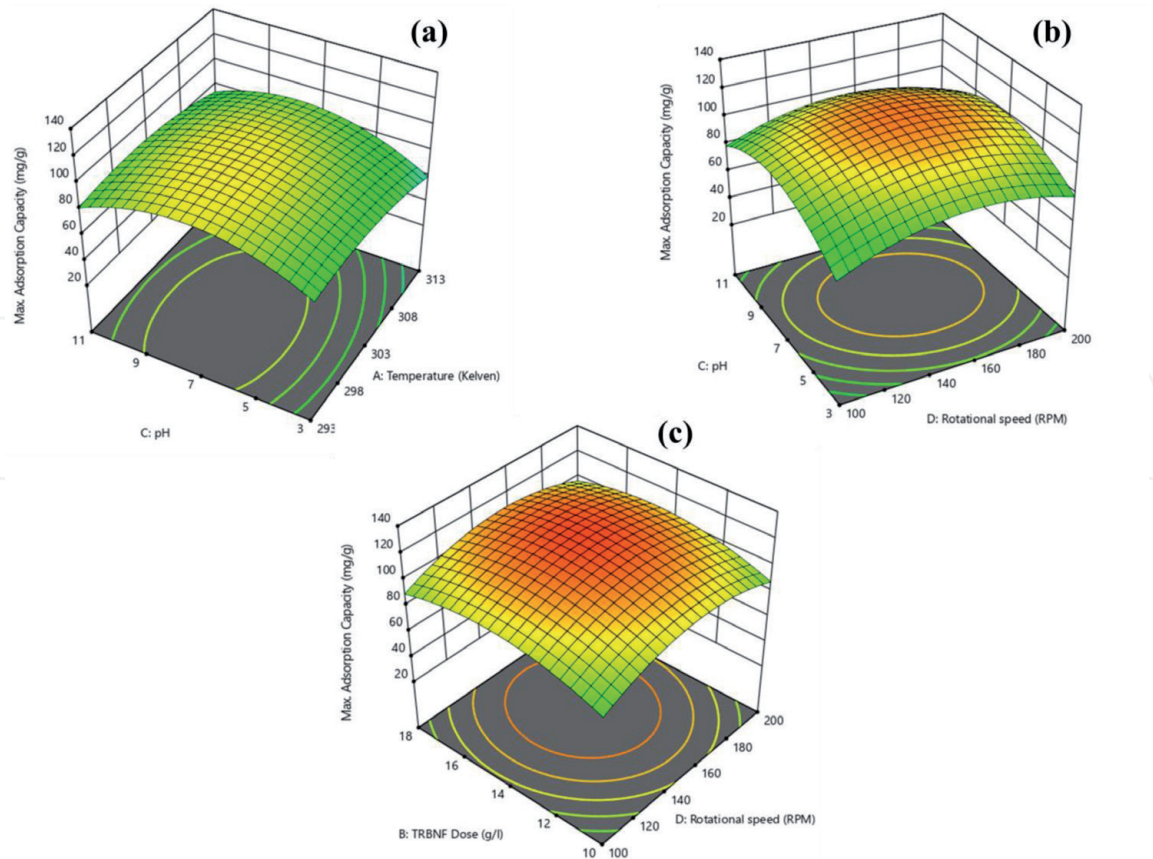


Figure 4. Surfaceplots obtains for Q_{max} (a) Temperature vs. pH; (b) Temperature vs. RPM; and (c) TRBNF dose Vs. RPM.

in the selected research domain by the adequate signal provided by the AP ratio. The developed response surface model shows the Maximum adsorption capacity as below,

$$\begin{aligned} \text{max. Adsorption Capacity} = & +124.10 - 4.36 A + 5.12 B + 2.12 C + 3.81 D \\ & + 0.6288 AB + 2.20 AC + 1.12 AD - 2.30 BC \quad (3) \\ & + 0.2462 BD - 1.93 CD - 8.07 A^2 - 12.95 B^2 \\ & - 20.42 C^2 - 15.94 D^2 \end{aligned}$$

Where, A, B, C and D are the coded factors (processing independent variables). The highest and the lowest levels of any particular coded factor are given as +1 and -1 respectively.

Moreover, **Figure 4(a)-(c)** depicts the approximated response surface plot for Q_{max} concerning the process parameters of solution pH, TRBNF dose, Temperature and RPM.

5. Optimization of the process variables based on desirability function analysis

Table 4 shows the various goals and ranges of process variables viz. pH, Temperature, TRBNF dose and rotational speed (RPM) and the response characteristics viz. Q_{max} . The aim of using the RSM desirability was to obtain the optimum processing condition by maximizing the desirability as 1. The range of desirability

Name	Goal	Lower Limit	Upper Limit	Lower Weight	Upper Weight	Importance
A:Temperature	is in range	293	313	1	1	3
B: pH.	is in range	3	11	1	1	3
C:TRBNF dose	is in range	10	18	1	1	3
D:RPM	is in range	100	200	1	1	3
Qmax	maximize	31.56	32.11	1	1	3

Table 4.
Limits of Input and output process parameters for DFA.

would be in between 0 to 1. 0 desirability value is practically impossible to obtained as it purely reliant on how the real optimum value are differ from the upper and lower point [22].

30 sets of the optimal solution are acquired for the specific design space constraints for Qmax using statistical Design Expert software11.0. The set of parametric conditions consisting of the maximum value of desirability is preferred as the optimal processing condition for the performance characteristics that are desired [22]. The **Table 5** depicts the highest desirability obtained along with the optimum desirability. After identifying the optimal processing condition, the subsequent step would be analysis the variation of performance measure obtains using optimal processing condition. Experimental measures have been taken place so as to ensure the verification of the predicted optimal setting of the input variables (pH, Temperature, TRBNF dose and rotational speed (RPM)). The deviation observed within the results obtained from the predicted optimal parameter settings and the experimental validation have been delineated in **Table 6**. It was found that the deviation was very minimal.

Figure 5(a) and **(b)** demonstrate the desirability ramp function and the bar graph respectively. The dot point on the ramp can be the measure of a particular variable within the specified experimental domain and the elevation would be responsible for how much desirable it is. The linear graph of ramp function obtained is demonstrating the weightage that how far the goal or target are from the high values and accordingly the weight factor is distributed as 1 [27].

Parameter	Goal	Optimum value
pH	in range	7.5
Temperature, (⁰ k)	in range	303
TRBNF dose, (g/l)	in range	15.1
Rotational speed, (RPM)	in range	158.5

Table 5.
Predicted optimum levels of process variables.

Responses	Goal	Predicted value	Observed value	Error (%)
Q _{max} (mg/g)	Maximize	32.11	31.56	1.71

Table 6.
Predicted and observed values of responses of Q_{max}.

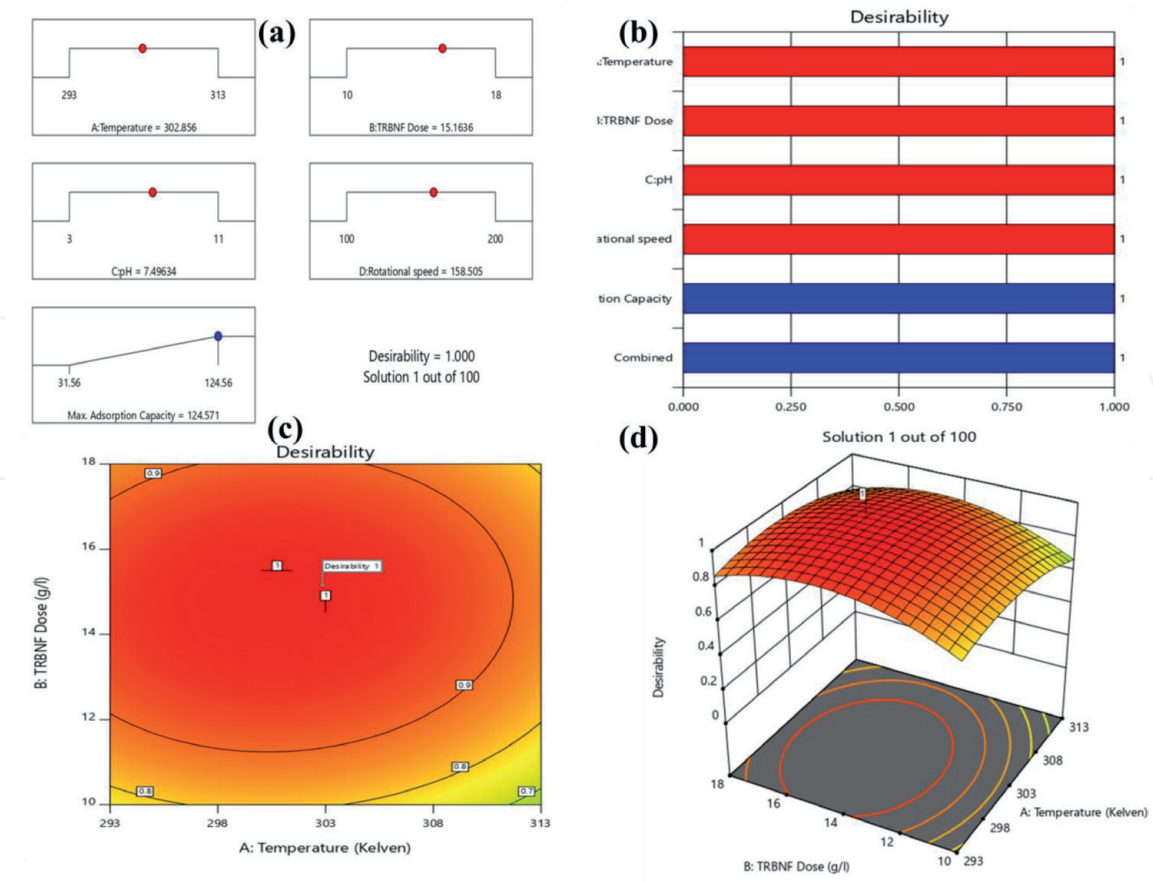


Figure 5. Ramp function plot of Desirability (a); Bar graph of Desirability (b); 3D Surface plot of desirability (c) 2D view (d).

The overall desirability of the performance characteristics have been demonstrated by the bar graph of desirability. The value has been chosen in between 0 to 1 depends on the proximity of the output towards the target. The value of desirability close to 1 is considered as acceptable.

As it is single response, the maximum weightage have been given to it and similar weighage have been given to all the input processing variables and a 3D desirability plot were drawn. **Figure 5C** and **D** demonstrates the desirability function distribution for Q max during varying the input responses. It can be observed that the value of overall desirability is less at a higher pulse current and pulse on-time region. The region for optimal desirability was placed near the topmost area of the plot, which shows the overall desirability value '1' that slowly decreased while moving to the right side and backwards. Hence, the elucidated desirability value of '1' illustrates the proximity of the response towards the target [22–26].

6. Adsorption mechanism

Understanding adsorption is the most important part of any study of adsorption. Due to this reason, it is important to understand two essential points, (1) The adsorbate structure and (2) To know the functional groups present in an adsorbent responsible for adsorption. In the present study for the adsorption of Methylene Blue (MB), the presence of amino groups in the dye results to the formation of hydrogen bond in between the amino group and the hydroxyl groups in TRBNF. The silica content was observed to decrease and the crystallinity of cellulose fraction was increases due to the treatment of ripe betel nut fibre by Na_2CO_3 results in changed surface morphology

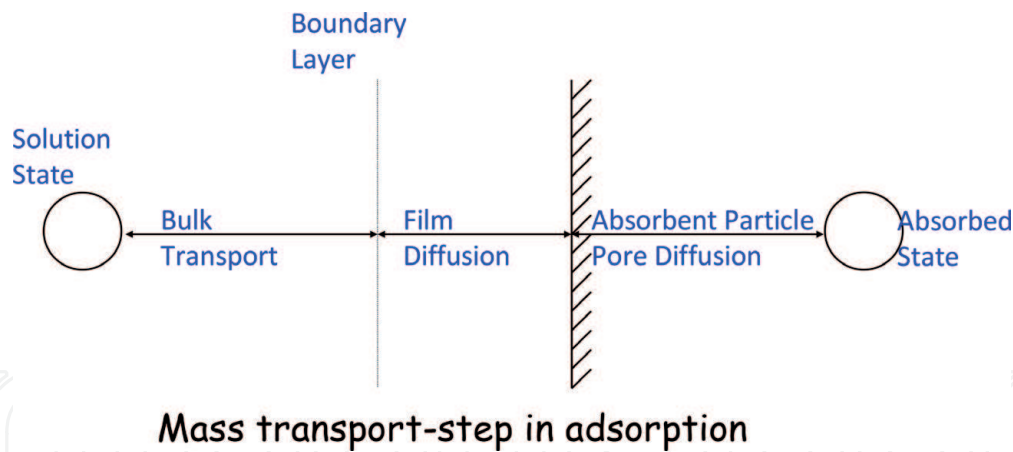


Figure 6.
General Mass transport step in adsorption.

of the betel nut fibre. The chances of chemical reaction to takes place between the hydroxyl exposed adsorbent and dye ions because of the changed surface morphology of the betel nut fibre and subsequently mechanical bonding takes place due to linkage of ions with the modified molecular structure of the absorbent.

As discussed in Section 5.6, during the first 60 minutes there was a very rapid rate of adsorption for all the cases, thereafter gradually slowed down and eventually, the equilibrium time reached 90 minutes revealing that the diffusion film has support the intra-particle diffusion. The maximum sorption was observed at pH value around 7.0. The primary adsorption mechanism were observed as below,

- The ripe betel nut fibre surface was absorbed the MB dye from the entire solution.
- The dye particles defused from aqueous solution to the adsorbent surface through the formation of boundary layer.
- The formation of Hydrogen bond between amino groups and the exposed hydroxyl group present in ripe betel nut fibres would be responsible for the successful adsorption by the of betel nut fibre. **Figure 6** delineated the general mass transfer phenomenon occurred in adsorption process.

7. Conclusions

In this study, ripe betel nut fibre treated with Na_2CO_3 was used as an adsorbent for the adsorption of Methylene Blue dye. For the design of the maximum adsorption capacity output, the usage of process parameters like pH, Temperature, TRBNF dose and RPM were successfully checked by using composite design face centred central response surface methodology by attending 30 experimental trials with repetition of three in each of the process parameters at three different levels. Results have shown that for optimum adsorption capacity, minimum to moderate temperature, moderate to high TRBNF dose and moderate RPM will be critical. The models are adequate which is proven by the obtained predicted value of R_2 for Q_{max} as 0.958. The result of Q_{max} was influenced by the two factors TRBNF dose and RPM. At moderate RPM and with an increase in TRBNF dose, the rate of adsorption increased. In this paper, the influence of all the process parameters is discussed. The combination of optimum parameter setting for Q_{max} obtained are pH 7.5,

Temperature, 303 K, TRBNF dose 15 gm/L and Rotational speed 158 RPM for maximizing the Q_{max} . The agreeable error percentage of 1.71 between the predicted and observed values for Q_{max} confirm the precision of the methodology.

IntechOpen

Author details

Amit Kumar Dey^{1*} and Abhijit Dey²

1 Department of Civil Engineering, Central Institute of Technology Kokrajhar, BTAD, Assam

2 Department of Mechanical Engineering, National Institute of Technology Srinagar, J&K, India

*Address all correspondence to: ak.dey@cit.ac.in

IntechOpen

© 2021 The Author(s). Licensee IntechOpen. This chapter is distributed under the terms of the Creative Commons Attribution License (<http://creativecommons.org/licenses/by/3.0>), which permits unrestricted use, distribution, and reproduction in any medium, provided the original work is properly cited. 

References

- [1] H. Zollinger. Colour Chemistry – Synthesis, Properties of Organic Dyes and Pigments. VCH Publishers, New York. (1987)92-100.
- [2] E.J. Weber, R.L. Adams, Chemical and sediment mediated reduction of the azo dye Disperse Blue 79. Environmental Science & Technology, 29 (1995) 1163-1170.
- [3] C. Wang, A. Yediler, D. Linert, Z. Wang, A. Kettrup, Toxicity evaluation of reactive dye stuff, auxiliaries and selected effluents in textile finishing industry to luminescent bacteria vibrio fisheri. Chemosphere, 46 (2002) 339-344.
- [4] E. Rindle, W.J. Troll, Metabolic reduction of benzidine azo dyes to benzidine in the Rhesus monkey. Journal of National Cancer Institute, 55 (1975)181.
- [5] Ali, R.; Zarei, M.; Moradkhannejhad, L. (2010) Application of response surface methodology for optimization of azo dye removal by oxalate catalyzed photoelectro-Fenton process using carbon nanotube-PTFE cathode. Desalination, 258: 112.
- [6] Chatterjee S.; kumarA.; Basu, S.; Dutta, S. (2012) Application of Response Surface Methodology for Methylene Blue dye removal from aqueous solution using low cost adsorbent. Chem. Eng. J, (181-182): 289.
- [7] Chen, Y.; Zhang, D. (2014) Adsorption kinetics, isotherm and thermodynamics studies of flavones from VacciniumbracteatumThunb leaves on NKA-2 resin. Chem. Eng. J, 254: 579.
- [8] Chiang, K. T. (2008) Modeling and analysis of the effects of machining parameters on the performance characteristics in EDM process of Al₂O₃ + TiC mixed ceramic. Int. J. Adv. Manuf. Technol, 37: 523.
- [9] Cho, Il-H.; Zoh, K. D. (2007) Photocatalytic degradation of azo dye (Reactive Red 120) in TiO₂/UV system: Optimization and modeling using a response surface methodology (RSM) based on the central composite design. Dye.Pigm, 75: 533.
- [10] Chong, M.N.; Jin, B.; Chow, C.W.K.; Saint, C.P. (2009) A new approach to optimize an annular slurry photoreactor system for the degradation of congo red: statistical analysis and modelling. Chem. Eng. J, 152: 158.
- [11] Chowdhury, S.; Mishra, R.; Saha, P.; Kuskwaha, P. (2011) Adsorption thermodynamics, Kinetics and isosteric heat of adsorption of malachite green onto chemically modified rice husk. Desalination, 265: 159.
- [12] Chowdhury, S.; Saha, P. (2010) Sea shell powder as a new adsorbent to remove Basic Green 4 (Malachite Green) from aqueous solutions: Equilibrium, kinetic and thermodynamic studies. Chem. Eng. J, 164: 168.
- [13] Reddy, D.H.K.; Yun, Y.S. (2016) Spinel ferrite magnetic adsorbents: alternative future materials for water purification. Coord. Chem. Rev., 315: 90.
- [14] Crini, G.; Peindy, H. N.; Gimbert, F.; Robert, C. (2007) Removal of C.I. Basic Green 4 (Malachite Green) from aqueous solutions by adsorption using cyclodextrin-based adsorbent: Kinetic and equilibrium studies. Separ.Purif. Technol, 53: 97.
- [15] Agarwal, A.; Singh, H.; Kumar, P.; Singh, M. (2008) Optimisation of power consumption for CNC turned parts using response surface methodology and Taguchi's technique – a comparative study. J. Mater. Proc. Technol, 200: 373.
- [16] Ali, R.; Zarei, M.; Moradkhannejhad, L. (2010) Application of response

surface methodology for optimization of azo dye removal by oxalate catalyzed photoelectro-Fenton process using carbon nanotube-PTFE cathode. *Desalination*, 258: 112.

[17] Chatterjee S.; kumar A.; Basu, S.; Dutta, S. (2012) Application of Response Surface Methodology for Methylene Blue dye removal from aqueous solution using low cost adsorbent. *Chem. Eng. J.*, (181-182): 289.

[18] Cho, Il-H.; Zoh, K. D. (2007) Photocatalytic degradation of azo dye (Reactive Red 120) in TiO₂/UV system: Optimization and modeling using a response surface methodology (RSM) based on the central composite design. *Dye.Pigm.*, 75: 533.

[19] Chong, M.N.; Jin, B.; Chow, C.W.K.; Saint, C.P. (2009) A new approach to optimize an annular slurry photoreactor system for the degradation of congo red: statistical analysis and modelling. *Chem. Eng. J.*, 152: 158.

[20] Ravikumar, K.; Krishnan, S., Ramalingam, S. (2007) Optimization of process variables by the application of response surface methodology for dye removal using a novel adsorbent. *Dye. Pigm.* 72: 66.

[21] Ravikumar, K.; Deebika, B.; Balu, K. (2005) Decolourization of aqueous dye solutions by a novel adsorbent: Application of statistical designs and surface plots for the optimization and regression analysis. *J. Hazar.Mater.*, 122: 75.

[22] Dey, A. K.; Dey, A. (2021) Selection of optimal processing condition during removal of Reactive Red 195 by NaOH treated jute fibre using adsorption, *Groundwater for Sustainable Development*, 12: 100522.

[23] Dey, A. K.; Kumar, U.; Dey, A.; (2018) Use of response surface methodology for the optimization of

process parameters for the removal of Congo Red by NaOH treated jute fibre, *.Desalination and Water Treatment*, 115: 300.

[24] Dey, A. K.; Kumar, U.; (2017) Adsorption of anionic azo dye Congo red from aqueous solution onto NaOH-modified jute fibre, *Desalination and Water Treatment*, 92:, 301.

[25] Dey, A. K.; Kumar, U. (2017) Adsorption of reactive red 195 from polluted water upon Na₂CO₃ modified jute fibre, *Int J Eng Technol*, 9: 53.

[26] Dey, A.; Pandey, K. M. (2018) Selection of optimal processing condition during WEDM of compocasted AA6061/cenosphere AMCs based on grey-based hybrid approach, *Mater. Manuf. Proc.*, 33(14): 1549.

[27] Rahman, M, ; Dey, A.; Pandey, K. M.; (2018) Machinability of cenosphere particulate–reinforced AA6061 aluminium alloy prepared by compocasting, *Proc. Inst. Mech. Eng. Part B: J. Eng. Manuf.*, 232(14): 2499.

[28] Dey, A.; Debnath, M.; Pandey, K. M. (2017) Analysis of effect of machining parameters during electrical discharge machining using Taguchi-based multi-objective PSO, *Int. J. Comp. Intel. App.*, 16 (02): 1750010.

[29] Niraj, N.; Pandey, K. M.; Dey, A. (2018) Tribological behaviour of Magnesium Metal Matrix Composites reinforced with fly ash cenosphere, *Mater. Today: Proc.*, 5(9): 20138.

[30] Dey, A.; Pandey, K. M. (2018) Wire electrical discharge machining characteristics of AA6061/cenosphere as-cast aluminum matrix composites, *Mater. Manuf. Proc.*, 33(12):1346.